VERSITA

CELLULAR & MOLECULAR BIOLOGY LETTERS
http://www.cmbl.org.pl

Received: 03 September 2014
Final form accepted: 29 January 2014
Published online: February 2014

Volume 19 (2014) pp 98-115
DOI: 10.2478/s11658-014-0183-7

Research article

NOVEL ESTRADIOL ANALOGUE INDUCES APOPTOSIS AND AUTOPHAGY IN ESOPHAGEAL CARCINOMA CELLS

ELIZE WOLMARANS[1], THANDI V. MQOCO[1], ANDRE STANDER[1], SANDRA D. NKANDEU[1], KATHERINE SIPPEL[2], ROBERT MCKENNA[3] and ANNIE JOUBERT[1,*]

[1]Department of Physiology, University of Pretoria, South Africa, [2]Department of Biochemistry and Molecular Biology, Baylor College of Medicine, Houston, Texas, USA, [3]McKnight Institute, University of Florida, Gainesville, Florida, USA

Abstract: Cancer is the second leading cause of death in South Africa. The critical role that microtubules play in cell division makes them an ideal target for the development of chemotherapeutic drugs that prevent the hyperproliferation of cancer cells. The new in silico-designed estradiol analogue 2-ethyl-3-O-sulfamoyl-estra-1,3,5(10)16-tetraene (ESE-16) was investigated in terms of its in vitro antiproliferative effects on the esophageal carcinoma SNO cell line at a concentration of 0.18 μM and an exposure time of 24 h. Polarization-optical differential interference contrast and triple fluorescent staining (propidium iodide, Hoechst 33342 and acridine orange) revealed a decrease in cell density, metaphase arrest, and the occurrence of apoptotic bodies in the ESE-16-treated cells when compared to relevant controls. Treated cells also showed an increase in the presence of acidic vacuoles and lysosomes, suggesting the occurrence of autophagic processes. Cell death via autophagy was confirmed using the Cyto-

* Author for correspondence. Email: annie.joubert@up.ac.za, phone: +27 12 319 2246, fax: +27 12 321 1679

Abbreviations used: 2ME – 2-methoxyestradiol; 2-MeOE2bisMATE – 2-methoxyestradiol-bis-sulfamate; AAF – aggresome activity factor; AIF – apoptosis inducing factor; AO – acridine orange; Apaf-1 – apoptosis protease-activating factor; C9 – 2-ethyl-3-O-sulfamoyl-estra-1,3,5(10)-tetraen-3-ol-17-one; CAII – carbonic anhydrase II; CAIX – carbonic anhydrase IX; DMEM – Dulbecco's modified Eagle's medium; DMSO – dimethyl sulfoxide; EC – esophageal cancer; ER – estrogen receptor; ESE-16 – 2-ethyl-3-*O*-sulfamoyl-estra-1,3,5(10)16-tetraene; FACS – fluorescence-activated cell sorting; FB1 – fumonisin B1; HO – Hoechst 33342; MFI – mean fluorescent intensity; MOMP – mitochondrial outer membrane permeabilization; PBS – phosphate buffer saline; PE – phosphatidylethanolamine; PI – propidium iodide; PlasDIC – polarization-optical transmitted light differential interference contrast microscopy; STS – steroid sulfatase

ID autophagy detection kit and the aggresome detection assay. Results showed an increase in autophagic vacuole and aggresome formation in ESE-16 treated cells, confirming the induction of cell death via autophagy. Cell cycle progression demonstrated an increase in the sub-G_1 fraction (indicative of the presence of apoptosis). In addition, a reduction in mitochondrial membrane potential was also observed, which suggests the involvement of apoptotic cell death induced by ESE-16 via the intrinsic apoptotic pathway. In this study, it was demonstrated that ESE-16 induces cell death via both autophagy and apoptosis in esophageal carcinoma cells. This study paves the way for future investigation into the role of ESE-16 in ex vivo and in vivo studies as a possible anticancer agent.

Keywords: Antiproliferative, 2-ethyl-3-*O*-sulfamoyl-estra-1,3,5(10)16-tetraene, ESE-16, Esophageal carcinoma, In vitro, Apoptosis, Autophagy

INTRODUCTION

Esophageal cancer (EC) is the eighth most common incident cancer in the world and due to its high fatality rate, it ranks sixth among all cancers in terms of mortality [1–3]. The highest rates of EC are found in Eastern Asia and Eastern and Southern Africa [4]. One of the main reasons for the high incidence rates in these areas is believed to be the presence of the mycotoxin fumonisin B1 (FB1). It occurs in high concentrations in the above-mentioned geographic areas due to a soil-borne fungus named *Fusarium verticillioides*, which frequently contaminates maize and maize products [5, 6]. Studies revealed that FB1 may act as a promoter or initiator of carcinogenesis in synergy with co-carcinogens such as the *N*-nitrosamines found in tobacco [6].

One of the best-known characteristics of cancer cells is their rapid and uncontrolled division. The critical role that microtubules play in cell division makes them an ideal target for the development of chemotherapeutic drugs that prevent the hyperproliferation of cancer cells [7]. Clinical success with several vinca alkaloids and taxanes on a wide variety of human cancers has proven the effectiveness of microtubule-targeting drugs and has prompted a worldwide search for compounds with similar mechanisms [7].

2-methoxyoestradiol (2ME) is an endogenous metabolite derived from 17β-estradiol (Fig. 1A) [7–12]. Research has shown that this compound has antiproliferative, anti-angiogenic and pro-apoptotic characteristics in vitro and in vivo [3, 7–9, 12–15]. 2ME causes abnormal mitotic spindle formation and mitotic accumulation in estrogen receptor-positive and -negative cells [9, 10, 13–16]. This causes the activation of the spindle assembly checkpoint leading to metaphase arrest. As a consequence, cell proliferation is inhibited and cell death is induced [9, 11, 17, 18]. 2ME is registered as Panzem by Entremed Inc. and is currently undergoing Phase I and II clinical trials [19–21]. However, it has low bioavailability due to rapid metabolic degradation by the enzyme 17β-hydroxysteroid dehydrogenase

type 2, found in the gastrointestinal tract and liver, prompting attempts to design promising anticancer analogues of 2ME [8, 22, 23].

One of the latest 2ME derivatives is the new in silico-designed compound 2-ethyl-3-*O*-sulfamoyl-estra-1,3,5(10)16-tetraene (ESE-16; Fig. 1B), which was designed in our laboratory after we identified potential carbonic anhydrase IX (CAIX) inhibitors, capable of interfering with microtubule dynamics [10]. Carbonic anhydrases are zinc enzymes that control the CO_2/bicarbonate ratio in the blood, and thus control the acid/base balance in the body [10, 24–26]. CAIX is overexpressed in a variety of tumors and contributes to the acidification of the extracellular environment of the tumors due to the conversion of carbon dioxide and water to carbonic acid [24, 27, 28]. The acidic environment promotes the expression of proteinases contributing to tumor growth, survival and metastasis [24, 27, 28].

A comparison of the chemical structures of ESE-16 and 2ME reveals an exchange of a sulfamoylated group for a hydroxyl group at position 3 and the removal of a hydroxyl group at position 17 on ESE-16 (Fig. 1A and B). The 2-methoxy-group of 2ME is of importance for drug activity, since it may enhance its antiproliferative characteristics [9, 29]. In addition, modification at the 3- and 17-positions may improve resistance to metabolism and increase the compound potency [9, 22, 29]. Sulfamoylation of 2ME is suggested to increase bioavailability, since these analogues are able to journey through the liver without undergoing presystemic metabolism [8, 10, 22, 30]. The latter characteristic is due to the ability of sulfamoylated derivatives to reversibly bind to the carbonic anhydrase II (CAII) found in erythrocytes [10, 31] causing the slow release of the compound into the blood stream, allowing the compound to bypass presystemic metabolism [10, 28, 31].

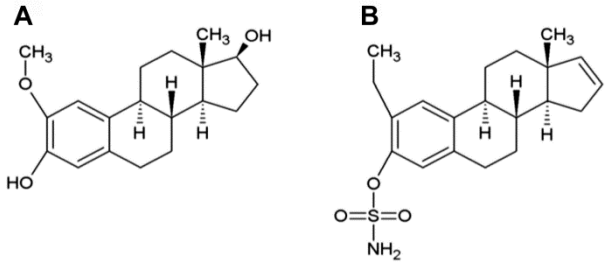

Fig. 1. The chemical structures of (A) 2-methoxyestradiol (2ME) and (B) 2-ethyl-3-*O*-sulfamoyl-estra-1,3,5(10)16-tetraene (ESE-16). A comparison of the chemical structures of ESE-16 and 2ME reveals a sulfamoylated group at position 3 and the absence of a hydroxyl group at position 17 of ESE-16 compared to 2ME (ACD/ChemSketch Freeware Version 12.01).

Our preliminary data showed that the antiproliferative effect of ESE-16 is more potent on malignant cell lines than on non-tumorigenic cells [32]. The selectivity of ESE-16 towards metastatic breast cancer cells (MDA-MB-231) and breast adenocarcinoma MCF-7 cells was demonstrated in a comparison to its behavior

toward non-tumorigenic MCF-12A cells [32]. The aim of this study was to establish whether ESE-16 inhibits cell proliferation via autophagy and apoptosis in esophageal carcinoma.

MATERIALS AND METHODS

Cell line

SNO esophageal carcinoma cells are non-keratinizing squamous epithelial cells supplied by Highveld Biological (Pty) Ltd. Dulbecco's modified Eagle's medium and Ham's F12 nutrient mixture, fetal calf serum, and sterile cell culture flasks and plates were obtained from Separations. Penicillin, streptomycin, fungizone, gentamycin and trypsin were obtained from Highveld Biological Ltd (Pty).

Reagents

Dimethyl sulfoxide (DMSO), propidium iodide (PI), Hoechst 33342 (HO) and acridine orange (AO) were supplied by Sigma-Aldrich Co. ESE-16 is not commercially available. It was developed in silico at the Bioinformatics and Computational Biology Unit at the University of Pretoria. The compound was synthesized by Ithemba Pharmaceuticals (Pty) Ltd.

Cell culture

SNO cells were maintained in 25-cm^2 tissue culture flasks and allowed to proliferate in DMEM with glucose, sodium pyruvate and L-glutamine in a humidified atmosphere at 37ºC with 5% CO_2.

General cell culture procedures

A stock solution of 10 mM ESE-16 dissolved in DMSO was diluted with medium to the desired concentration prior to exposure of the cells. The concentration of 0.18 μM for ESE-16 was chosen since previous dose-dependent investigations conducted in our laboratory showed ESE-16 inhibiting cell proliferation to 50% at concentrations ranging from 0.18 μM to 0.22 μM [10]. After seeding, cells were incubated for 24 h in a humidified atmosphere (37ºC with 5% CO_2), to allow for attachment. This was then followed with 24 h exposure under the same conditions.

Appropriate controls were included: cells propagated in growth medium only; and a vehicle control composed of cells treated with DMSO with a final dilution never exceeding 0.02% (v/v) [32, 33]. Actinomycin D (0.1 μg/ml in growth medium) was used as a positive control for the induction of apoptosis [33]. To induce autophagy, cells were starved in a mixture with a 1:2 ratio of growth medium to phosphate buffer saline (PBS) [33].

Polarization-optical differential interference contrast microscopy (PlasDIC)

PlasDIC is an improved polarization-optical transmitted light differential interference contrast method that allows linearly polarized light to be generated

only after the objective [12, 31, 34]. PlasDIC provides high-quality imaging of cells in plastic cell culture vessels. Cells were photographed before and after exposure to obtain qualitative data. Qualitative analysis via PlasDIC images was repeated three times and one set of representative data is shown.

Triple fluorescent staining and fluorescence microscopy

This method was used to provide information on cell viability and to determine whether there was any induction of cell death (apoptosis, autophagy or necrosis). HO is a fluorescent dye that penetrates cells with an intact cell membrane (which includes viable cells and cells undergoing apoptosis) and fluoresces nuclei blue [35]. PI only penetrates cells that have lost their membrane integrity and is thus used to fluoresce oncotic or necrotic processes red. AO is a lysosomotropic fluorescent compound used to stain acidic vesicular organelles bright green in cells undergoing autophagy [35, 36].

SNO cells were seeded into a 6-well plate in complete growth medium with 2.5 x 10^5 cells per well and were subsequently exposed to ESE-16. Applicable controls were added as previously described. After the incubation periods, 0.5 ml of HO was added to the medium and incubated for 30 min at 37ºC. After 25 min of incubation, 0.5 ml of AO and 0.5 ml of PI were added and cells were incubated at 37ºC for another 5 min. The medium was discarded and the cells were washed twice with PBS.

Cells were examined with a Zeiss inverted Axiovert CFL40 microscope and Zeiss Axiovert MRm monochrome camera. Zeiss filter 2 was used for HO-stained cells (blue), Zeiss filter 9 for AO-stained cells (green) and Zeiss filter 15 for PI-stained cells (red). All of the procedures were performed with the plates and reagents covered with foil to prevent quenching of the fluorescent dye. This experiment was performed twice and representative data of one repeat is shown.

Flow cytometry

Cyto-ID autophagy detection kit. The Cyto-ID autophagy detection kit (Enzo Life Sciences) measures the presence of autophagic vacuoles and monitors autophagic flux in live cells using a dye that selectively labels autophagic vacuoles. The dye exhibits bright fluorescence upon incorporation into pre-autophagosomes, autophagosomes and autolysosomes.

Cells were seeded at 1 x 10^6 cells per 25-cm^2 flask in complete growth medium and were exposed ESE-16. Applicable controls were included as previously described. After the incubation periods, the termination procedure was followed [37]. Cells were trypsinized and samples were centrifuged at 400 x g for 5 min. The supernatant was removed and the cell pellet was resuspended in 2 ml of PBS and centrifuged at 400 x g for 5 min. The supernatant was removed and the cell pellet was resuspended in 500 µl of freshly diluted CytoID green detection reagent. Samples were incubated for 30 min in the dark at 37ºC and were subsequently analyzed in the FL1 channel of a fluorescence-activated cell sorting (FACS) FC500 System flow cytometer equipped with an air-cooled argon laser excited at 488 nm supplied by Beckman Coulter South Africa (Pty)

Ltd. This experiment was repeated three times with at least 10,000 to 30,000 events counted for each repeat. Data were analyzed using the Cyflogic program created by Pertu Terho and Mika Korkeamäki from CyFlo Ltd.

Aggresome detection kit. The proteostat aggresome detection assay (Enzo Life Sciences) was used [38] to determine whether ESE-16 causes aggresome formation within the SNO cells as an indication of autophagic cell death [39–41]. The assay was developed to detect aggregated proteins by means of a fluorescent molecular rotor dye. The mean fluorescent intensity (MFI) values obtained via flow cytometry were used to calculated the aggresome activity factor (AAF; Formula 1). According to the supplier's manual an AAF value greater than 25 indicates aggresome formation.

$$\mathrm{AAF} = \frac{100 \times (\mathrm{MFI}_{\mathrm{TREATED}} - \mathrm{MFI}_{\mathrm{CONTROL}})}{\mathrm{MFI}_{\mathrm{TREATED}}} \quad (1)$$

Cells were seeded at 5 x 10^5 cells per 25-cm^2 flask in complete growth medium and subsequently exposed to ESE-16. Applicable controls were included as previously described. After the incubation periods, the cells were trypsinized and centrifuged at 400 x g for 5 min and the supernatant was removed. Samples were fixed by adding 2 ml of 4% formaldehyde solution dropwise to the cell pellet while slowly vortexing. Incubation was at room temperature for 30 min.
The samples were then centrifuged at 800 x g for 10 min and the supernatant was removed. Washes were performed by adding 2 ml 1 x Assay Buffer. The washed samples were centrifuged at 800 x g for 10 min and the supernatant was removed. Permeabilization was achieved by the dropwise addition of 2 ml permeablizing solution while slowly vortexing and incubated for 30 min on ice.
The samples were subsequently centrifuged at 800 x g for 10 min. The supernatant was removed and the samples were washed by resuspending the cell pellet with 2 ml 1 x Assay Buffer. The samples were centrifuged at 800 x g for 10 min, the supernatant was discarded, and staining was performed by resuspending the cell pellet in 500 µl of freshly diluted ProteoStat Aggresome Red Detection Reagent. Samples were protected from light, incubated for 30 min at room temperature, and analyzed in the FL3 channel of a FACS FC500 System flow cytometer equipped with an air-cooled argon laser excited at 488 nm (Beckman Coulter South Africa (Pty) Ltd). This experiment was repeated three times with at least 10,000 to 30,000 events being counted for each repeat. Data were analyzed using the Cyflogic program (CyFlo Ltd).

Cell cycle analysis. Cell cycle analysis was performed to view cell cycle progression and DNA integrity. The analysis was conducted via PI staining of the cells to determine the amount of DNA present [10]. Cells were seeded at 750,000 cells per 25-cm^2 flask in complete growth medium and were subsequently exposed to ESE-16. Applicable controls were included as previously described. After the incubation periods, cells were trypsinized and

samples were centrifuged at 400 x g. The supernatant was removed and the cell pellet was resuspended in 1 ml ice-cold PBS. Cells were centrifuged at 400 x g and the supernatant was removed. The samples were then fixed by resuspending the cell pellet in 200 µl ice-cold PBS containing 0.1% fetal bovine serum. Ethanol (70%; 4 ml) was added dropwise to the solution with vortexing. The samples were left at 4ºC overnight.

After fixation, the samples were centrifuged and the supernatant was removed. The cell pellet was resuspended in PBS containing PI (40 µg/ml), RNAse (100 µg/ml) and 0.1% Triton X-100. Incubation was at 37ºC with 5% CO_2 for 40 min. Fluorescence was measured by using the FL3 channel of a FACS FC500 System flow cytometer equipped with an air-cooled argon laser excited at 488 nm (Beckman Coulter South Africa (Pty) Ltd). This experiment was repeated three times with at least 10,000 to 30,000 events being counted for each repeat and analysis of the data were conducted by using the Cyflogic program (CyFlo Ltd).

Mitochondrial membrane potential. The MitoTracker kit (Biocom Biotech Pty Ltd) [42] was used to test whether ESE-16 influences the mitochondrial membrane potential of SNO cells. The mitochondria are labeled using a cationic dye named 5,5',6,6'-tetrachloro-1,133'-tetra-ethylbenzimidazolyl-carbocyanine iodide, which passively diffuses across the plasma membrane and accumulates in active mitochondria, providing red fluorescence [31]. However, if there is a reduction in the mitochondrial membrane potential, the dye cannot aggregate in the mitochondria and remains in the cytoplasm in its monomer form, generating green instead of red fluorescence [31].

Cells were seeded in complete growth medium at 500,000 cells per 25-cm^2 flask and were subsequently exposed to ESE-16. Applicable controls were included as previously described. After the incubation periods, cells were trypsinized and centrifuged at 13,000 x g. The supernatant was removed, the cell pellet was resuspended in 1 ml of diluted MitoCapture solution and samples were incubated in a humidified atmosphere (37ºC and 5% CO_2) for 20 min. After the incubation period, samples were centrifuged at 500 x g, the supernatant was removed and cells were resuspended in 1 ml of pre-warmed (37ºC) incubation buffer. Cells were analyzed using a FACS FC500 System flow cytometer equipped with an air-cooled argon laser excited at 488 nm (Beckman Coulter South Africa (Pty) Ltd). Apoptotic cells were detected in the FITC channel (FL1) showing diffused green fluorescence. Healthy cells were detected in the propidium iodide channel (FL2) showing red fluorescence. This experiment was repeated three times with at least 10,000 to 30,000 events being counted for each repeat. Data were analyzed using the Cyflogic program (CyFlo Ltd).

Statistical analysis of data

Qualitative analysis was conducted via PlasDIC and triple fluorescent staining. PlasDIC was repeated three times and triple fluorescent staining was repeated twice. Quantitative analysis of cell cycle progression, aggresome detection and mitochondrial membrane potential with the use of flow cytometry were each

repeated three times. In addition, at least 10,000 to 30,000 events were counted for each repeat. Data were analyzed using the Cyflogic program created by Pertu Terho and Mika Korkeamäki from CyFlo Ltd. Statistical analysis of all of the results obtained was determined by using Student's *t*-test and a p-value of less thn 0.05 was accepted as significant.

RESULTS

Qualitative data reveal a decrease in cell density and cell death via apoptosis and autophagy

PlasDIC was used to visualize the effect that 0.18 μM of ESE-16 has on SNO cell morphology after 24 h of exposure. Cells treated with ESE-16 (Fig. 2D) showed a decrease in cell density, the occurrence of membrane blebbing, and the presence of apoptotic bodies when compared to the relevant controls (Fig. 2A–C). An increase in the number of cells in mitosis, indicative of cells in a metaphase block, was also observed.

Triple fluorescent staining with HO, PI and AO was used to determine possible induction of apoptosis and autophagy after 24 h of exposure to 0.18 μM of ESE-16. HO penetrates a cell with an intact cell membrane, which includes viable cells and cells undergoing apoptosis, and fluoresces the nuclei blue [35]. PI only penetrates cells that have lost their membrane integrity and is thus used to fluoresce oncotic or necrotic processes red. AO is a lysosomotropic fluorescent compound used to stain acidic vesicular organelles bright green in cells undergoing autophagy [35, 36]. Results revealed a decrease in cell density, metaphase arrest, and the occurrence of apoptotic bodies in ESE-16-treated cells (Fig. 3D) when compared to the relevant controls (Fig. 3A–C). ESE-16-treated cells and starved cells (positive control for autophagy; Fig. 3C) showed an increase in green fluorescence due to the presence of acidic vacuoles and lysosomes, suggesting the occurrence of autophagic processes. Results obtained with triple fluorescent staining suggested that ESE-16 caused both autophagic and apoptotic cell death.

Quantitative confirmation of autophagic cell death occurring after exposure to ESE-16

The Cyto-ID Autophagy Detection Kit (Enzo Life Sciences) measures autophagic vacuoles and monitors autophagic flux in live cells using a novel dye that selectively labels autophagic vacuoles. The excitable green fluorescence detection reagent becomes brightly fluorescent when incorporated into pre-autophagosomes, autophagosomes and autolysosomes. It was used to monitor autophagic flux in the SNO cells. The results showed a shift to the right in the histogram representing the ESE-16-treated cells when compared to the vehicle control (Fig. 4A). The shift to the right indicates an increase in fluorescence, demonstrating an increase in the number of autophagic vacuoles in ESE-16-

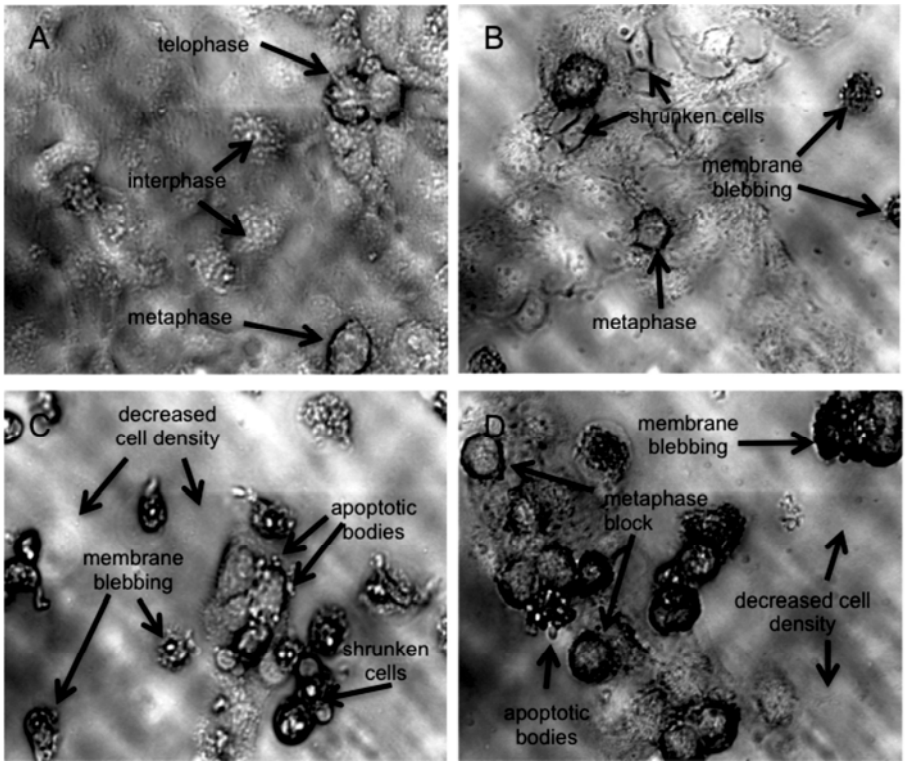

Fig. 2. Polarization-optical differential interference contrast (PlasDIC) images of SNO cells after exposure to ESE-16 and various controls. A – DMSO-treated cells (vehicle control). B – Starved cells. C – Actinomycin D-treated cells. D – ESE-16-treated cells after an exposure period of 24 h (40x magnification). ESE-16-treated cells showed a decrease in cell density along with morphological indicators of apoptosis (membrane blebbing and apoptotic bodies). An increase in the number of cells in metaphase was also observed. Similar apoptotic morphology was observed in the actinomycin D-treated cells (positive control for apoptosis). The positive control for autophagy (starved cells), showed a decrease in cell density and cells were shrunken. The vehicle control sample showed normal cell morphology.

treated cells. These results confirm the qualitative data obtained from the triple fluorescent staining images.

Possible aggresome formation (another indication of the presence of autophagy) was also determined in ESE-16-treated SNO cells using an Aggresome Detection Kit. According to the supplier's manual, the assay is developed to detect aggregated proteins by means of a fluorescent molecular rotor dye. The AAF was calculated using Formula 1 and the mean MFI values obtained via flow cytometry. The results showed a shift to the right in the histogram for the ESE-16-treated cells (Fig. 4B), which illustrates a higher MFI in ESE-16-treated samples when compared to the vehicle control. This indicates an increase in aggresome formation in the ESE-16-treated cells confirming the presence of autophagy in the ESE-16-treated cells.

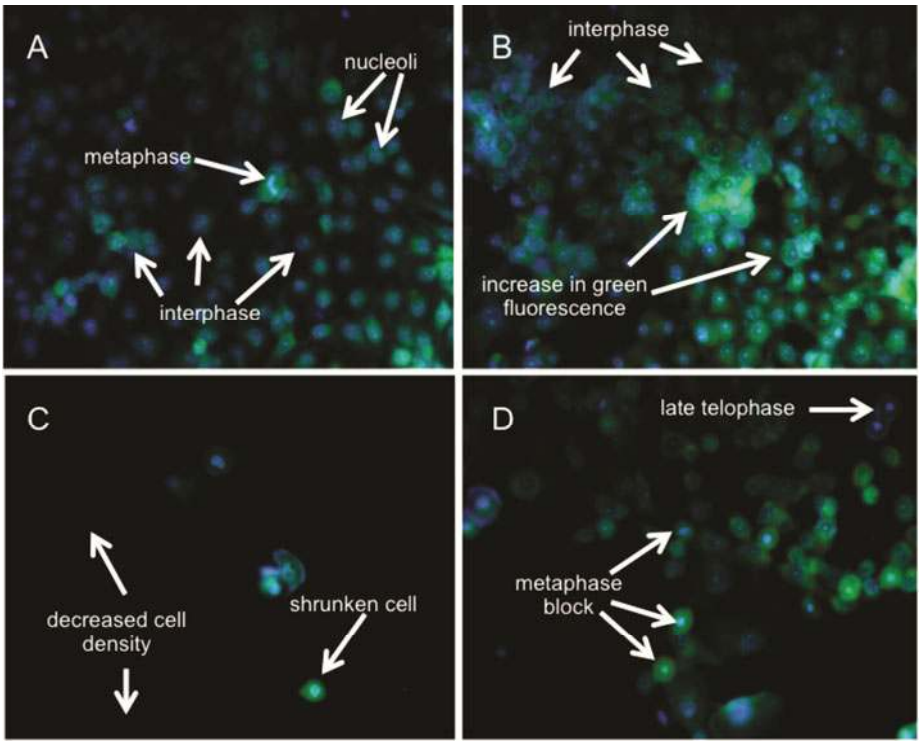

Fig. 3. Triple-stained images of SNO cells after exposure to ESE-16 and various controls. A – DMSO-treated cells (vehicle control). B – Starved cells. C – Actinomycin D-treated cells. D – ESE-16-treated cells (20x magnification). ESE-16 treated cells showed a decrease in cell density along with morphological indicators of apoptosis, such as membrane blebbing and apoptotic bodies. An increase in the number of cells in metaphase was also observed together with an increase in green fluorescence in the ESE-16-treated cells. The increase in green fluorescence (also observed in starved cells) is indicative of an increase in acidic vacuoles and lysosomal activity, which is characteristically found in cells undergoing autophagy. Actinomycin D-treated cells showed a decrease in cell density, whereas the vehicle control revealed normal cell morphology in cells treated with DMSO.

Quantitative confirmation of apoptotic cell death occurring after exposure to ESE-16

Cell cycle analysis was performed to view the influence of ESE-16 on cell cycle progression. An increase in the percentage of cells in sub G_1 (indicative of apoptosis) in the ESE-16-treated cells was observed when compared to the relevant controls (Fig. 5). This confirms the qualitative data observed in the PlasDIC images.

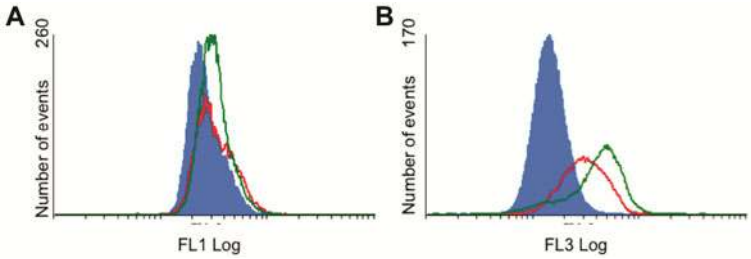

Fig. 4. Representative histograms illustrating the occurrence of autophagy in SNO cells after exposure to ESE-16. A – Cyto-ID Quantification. A representative histogram illustrating the increase in MFI [36] in the ESE-16-treated cells (the red histogram) compared to the vehicle control (the blue histogram). For this repeat, the vehicle control had an X-mean of 29.6 while cells treated with ESE-16 had an X-mean of 37.05. The green histogram represents the positive control for autophagy (cells starved with PBS) and had an X-mean of 35.51. [37]. B – Aggresome formation. A representative histogram illustrating the increase in MFI [38] by the ESE-16-treated cells (red histogram) compared to the vehicle control (blue histogram). The vehicle control had an X-mean of 16.65, while the ESE-16-treated cells had an X-mean of 36.21. The calculated AAF was determined as 54.02; indicating an increase in aggresome formation. The green histogram represents starved cells and had an X-mean of 47.9.

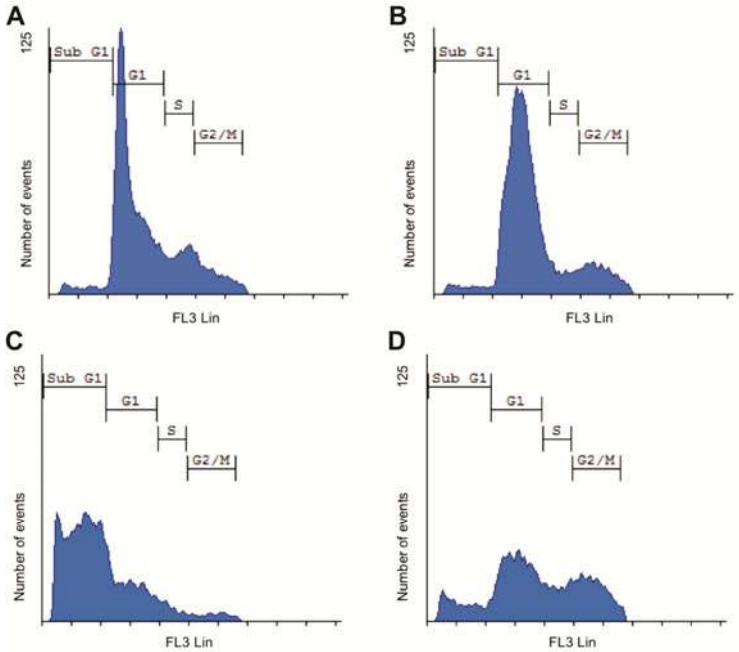

Fig. 5. Representative histograms illustrating the cell cycle progression of SNO cells after exposure to ESE-16 and various controls. A – DMSO-treated cells (vehicle control). B – Starved cells. C – Actinomycin D-treated cells. D – ESE-16-treated cells. The percentage of cells in sub G_1 among the ESE-16-treated cells was found to be 9.82%, which is statistically significantly higher compared to the 2.80% of cells in sub G_1 among the vehicle-treated control cells. An increase in the percentage of cells in the G_2/M phase in the ESE-16-treated samples was also found compared to the vehicle control (see Table 1).

Table 1. Percentage of cells in the different phases of the cell cycle of the ESE-16-treated samples and the relevant controls of the representative repeat.

	DMSO	Starved	Actinomycin	ESE-16
Sub G_1	2.8%	2.96%	55.59%	9.82%
G_1	66.21%	73.29%	36.14%	42.8%
S	10.49%	6.09%	5.28%	11.56%
G_2/M	20.61%	17.75%	6.68%	36.1%

The MitoTracker kit (Biocom Biotech Pty Ltd) [42] was used to test whether ESE-16 influences the mitochondrial membrane potential [42]. The mitochondria are labelled using a cationic dye named 5,5',6,6'-tetrachloro-1,133'-tetra-ethylbenzimidazolyl-carbocyanine iodide, which passively diffuses across the plasma membrane and accumulates in active mitochondria. Reduction of the mitochondrial membrane potential is an early feature of apoptosis due to loss of the electrochemical gradient across the mitochondrial membrane. With the reduction of the mitochondrial membrane potential, the MitoTracker dye cannot aggregate in the mitochondria and remains in the cytoplasm in its monomer form, generating green fluorescence [31]. The results show an increase in green fluorescence in the ESE-16-treated cells when compared to the relevant controls (Fig. 6). The results illustrate that ESE-16 causes a decrease in mitochondrial membrane potential that may lead to the degradation of the mitochondrial membrane and apoptosis. These findings once again confirm the qualitative data observed in the PlasDIC images.

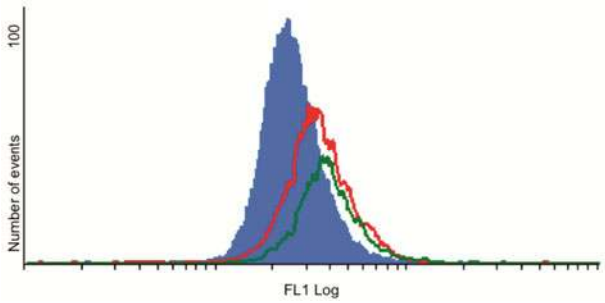

Fig. 6. Representative histogram illustrating the change in mitochondrial membrane potential in SNO cells after exposure to ESE-16. The shift to the right by the ESE-16-treated cells indicates an increase in green fluorescence indicative of decreased mitochondrial membrane potential. The blue graph represents the vehicle treated cells with an X-mean of 28.19. The red graph represents the ESE-16-treated cells which had an X-mean of 39.13. The green graph represents the positive control for apoptosis (cells treated with actinomycin D) with an X-mean of 43.85.

DISCUSSION

Researchers have previously documented that 2ME has antiproliferative, anti-angiogenic and pro-apoptotic characteristics in vitro and in vivo [3, 7–9, 13, 14, 22]. However, due to its low bioavailability [8, 22] attempts have been made to create analogues with improved bioavailability and potency. A new estradiol analogue, ESE-16, a sulfamoylated derivate of 2ME, was in silico-designed in our laboratory [10].

This article reports on the first investigation conducted on the antiproliferative influence of this novel compound on the esophageal carcinoma SNO cell line, a cell line chosen due to the high rates of esophageal cancer in South Africa [4]. Qualitative and quantitative data of this study suggest that this compound inhibits proliferation of the SNO cells and induces cell death via both the apoptotic and autophagic cell death pathways.

PlasDIC imaging showed a decrease in cell density and cells showing hallmarks of apoptosis, which included cell shrinkage, cell membrane blebbing, and the presence of apoptotic bodies. An increased number of cells in metaphase with hypercondensed chromatin in the ESE-16-treated cells were also visible. The increased number of cells in metaphase among the ESE-16-treated cells suggests abnormal mitotic spindle formation and mitotic accumulation leading to metaphase arrest and cell death [3, 9–11, 13–17]. This mechanism of cell death is similar to that seen with 2ME [9, 10, 13–16]. ESE-16 is also more potent than 2ME, showing a nanomolar GI_{50} value [10].

The occurrence of apoptosis was confirmed via the presence of a sub G_1-fraction and reduced mitochondrial membrane potential implicated apoptotic activation via the intrinsic apoptotic pathway. The increase in the G_2/M phase indicates an increase in cells in metaphase arrest [42].

Triple fluorescent staining revealed an increase in lysosomal activity in cells treated with ESE-16 when compared to relevant controls suggesting the presence of autophagic processes together with apoptosis. To confirm the presence of autophagy, the Cyto-ID autophagy detection kit and the aggresome detection assays were used to provide evidence for the presence of autophagy induction by ESE-16 in SNO cells.

Several types of cell death exist, each characterized by distinct morphological features and regulated and executed by different signaling pathways [43]. Apoptosis is characterized by chromatin condensation and fragmentation, membrane blebbing and disintegration of the cell into apoptotic bodies [43, 44]. Mitochondria play a key role in the signal transduction of apoptotic cell death [44]. Mitochondrial membrane permeabilization (MMP) affects the inner mitochondrial membrane (IM) and outer mitochondrial membrane (OM) [44, 46]. IM permeabilization disrupts the mitochondrial ion and volume homeostasis leading to the dissipation of the mitochondrial inner transmembrane potential ($\Delta\Psi m$) [45–47]. OM permeabilization leads to the release of several pro-apoptotic proteins such as apoptosis-inducing factor (AIF) and cytochrome *c* [44–46].

Autophagy is a process in which the intracellular contents are engulfed and consumed by vesicles, known as autophagosomes [43, 45]. The autophagosomes fuse with lysosomes to form autolysosomes, in which the components are degraded by lysosomal hydrolases [46]. Aggresome formation can also be used to monitor autophagy, since the aggresome serves as a storage compartment for protein aggregates and can be actively involved in their degradation with the help of autophagic clearing [47].

Despite marked differences between apoptosis and autophagy, recent studies have suggested that there is crosstalk between the autophagic and apoptotic pathways [48, 49]. Studies indicated that components of the core regulating apoptotic machinery can control autophagy with other studies showing autophagy regulators capable of controlling apoptosis [49]. It has been found that some connections occur upstream of the autophagic and apoptotic machinery which can be triggered by upstream signals resulting in combined autophagy and apoptosis or the cells switching between the two types of cell death in a mutually exclusive manner [48–50]. This illustrates that the apoptotic and autophagic response machineries share common pathways that either link or polarize the cellular responses [50].

CONCLUSION

This study is the first to demonstrate that the new in silico-designed compound ESE-16 has an antiproliferative effect on the esophageal carcinoma SNO cell line. Data established the ability of ESE-16 to induce both apoptotic and autophagic cell death at a concentration of 0.18 μM with an exposure time of 24 h. Results showed apoptotic cell death induction by ESE-16 is mediated via mitochondrial depolarization. Furthermore, the induction of autophagy in the ESE-16 treated cells revealed a functional relationship between the two types of cell death. Continuing research in this field will focus on understanding the biochemical pathways activated by this unique compound, which will pave the way for ex vivo and in vivo studies of ESE-16 as a possible anticancer agent.

Acknowledgements. Most of the experiments were conducted at the Department of Physiology, University of Pretoria, South Africa. Flow cytometry was conducted at the Department of Pharmacology, University of Pretoria, South Africa. This study was supported by grants from the Medical Research Council of South Africa, the Cancer Association of South Africa, Research Committee of the University of Pretoria (RESCOM), the National Research Foundation (NRF), the Institute of Cellular and Molecular Medicine (ICMM), and the Struwig-Germeshuysen Cancer Research Trust of South Africa.

REFERENCES

1. Kamangar, F., Dores, G.M. and Anderson, W.F. Patterns of cancer incidence, mortality, and prevalence across five continents: defining priorities to reduce cancer disparities in different geographic regions of the world. **J. Clin. Oncol.** 24 (2006) 2137–2150.
2. Kamangar, F., Chow, W.H., Abnet, C.C. and Dawsey, S.M. Environmental causes of esophageal cancer. **Gastroenterol. Clin. North Am.** 38 (2009) 27–57.
3. Du, B., Zhao, Z., Sun, H., Ma, S., Jin, J. and Zhang, Z. Effects of 2-methoxyestradiol on proliferation, apoptosis and gene expression of cyclin B1 and c-Myc in esophageal carcinoma EC9706 cells. **Cell. Biochem. Funct.** 30 (2012) 158–165.
4. Jemal, A., Bray, F., Center, M.M., Ferlay, J., Ward, E. and Forman, D. Global Cancer Statistics. **CA Cancer J. Clin.** 61 (2011) 69–90.
5. Chu, F.S. and Li, G.Y. Simultaneous occurrence of fumonisin B1 and other mycotoxins in moldy corn collected from the People's Republic of China in regions with high incidences of esophageal cancer. **Appl. Environ. Microbiol.** 60 (1994) 847–852.
6. Myburg, R.B., Dutton, M.F. and Chuturgoon, A.A. Cytotoxicity of fumonisin B1, diethylnitrosamine, and catechol on the SNO esophageal cancer cell line. **Environ. Health Perspect.** 110 (2002) 813–815.
7. Zhou, J. and Giannakakou, P. Targeting microtubules for cancer chemotherapy. **Curr. Med. Chem. Anticancer Agents** 5 (2005) 65–71.
8. Purohit, A., Hejaz, H.A., Walden, L., MacCarthy-Morrogh, L., Packham, G., Potter, B.V. and Reed, M.J. The effect of 2-methoxyoestrone-3-O-sulfamate on the growth of breast cancer cells and induced mammary tumors. **Int. J. Cancer** 85 (2000) 584–589.
9. Chua, Y.S., Chua, Y.L. and Hagen, T. Structure activity analysis of 2-methoxyestradiol analogues reveals targeting of microtubules as the major mechanism of antiproliferative and proapoptotic activity. **Mol. Cancer Ther.** 9 (2010) 224–235.
10. Stander, A., Joubert, F. and Joubert, A. Docking, synthesis, and in vitro evaluation of antimitotic estrone analogs. **Chem. Biol. Drug Des.** 77 (2011) 173–181.
11. Choi, H.J. and Zhu, B.T. Critical role of cyclin B1/Cdc2 up-regulation in the induction of mitotic prometaphase arrest in human breast cancer cells treated with 2-methoxyestradiol. **Biochim. Biophys. Acta** 1823 (2012) 1306–1315.
12. Visagie, M., Mqoco, T. and Joubert, A. Sulphamoylated estradiol analogue induces antiproliferative activity and apoptosis in breast cell lines. **Cell. Mol. Biol. Lett.** 17 (2012) 549–558.
13. Mooberry, S.L. Mechanism of action of 2-methoxyestradiol: new developments. **Drug Resist. Updat.** 6 (2003) 355–361.

14. Zhu, B.T. and Conney, A.H. Is 2-methoxyestradiol an endogenous estrogen metabolite that inhibits mammary carcinogenesis? **Cancer Res.** 58 **(**1998) 2269–2277.
15. Mabjeesh, N.J., Escuin, D., LaVallee, T.M., Pribluda, V.S., Swartz, G.M., Johnson, M.S., Willard, M.T., Zhong, H., Simons, J.W. and Giannakakou, P. 2ME2 inhibits tumor growth and angiogenesis by disrupting microtubules and dysregulating HIF. **Cancer Cell** 3 (2003) 363–375.
16. Thaver, V., Lottering, M., van Papendorp, D. and Joubert, A. In vitro effects of 2-methoxyestradiol on cell numbers, morphology, cell cycle progression, and apoptosis induction in oesophagealcarcinoma cells. **Cell Biochem. Funct.** 27 (2009) 205–210.
17. Van Zijl, C., Lottering, M.L., Steffens, F. and Joubert, A. In vitro effects of 2-methoxyestradiol on MCF-12A and MCF-7 cell growth, morphology and mitotic spindle formation. **Cell Biochem. Funct.** 26 (2008) 632–642.
18. Voster, C.J.J. and Joubert, A.M. In vitro effects of 2-methoxyestradiol-bis-sulfamate on the non-tumorigenic MCF-12A cell line. **Cell Biochem. Funct.** 28 (2010) 412–419.
19. Bruce, J.Y., Eickhoff, J., Pili, R., Logan, T., Carducci, M., Arnott, J., Treston, A., Wilding, G. and Liu, G. A phase II study of 2-methoxyestradiol nanocrystal colloidal dispersion alone and in combination with sunitinib malate in patients with metastatic renal cell carcinoma progressing on sunitinib malate. **Invest. New Drugs** 30 (2012) 794–802.
20. Harrison, M.R., Hahn, N.M., Pili, R., Oh, W.K., Hammers, H., Sweeney, C., Kim, K., Perlman, S., Arnott, J., Sidor, C., Wilding, G. and Liu, G. A phase II study of 2-methoxyestradiol (2ME2) NanoCrystal dispersion (NCD) in patients with taxane-refractory, metastatic castrate-resistant prostate cancer (CRPC). **Invest. New Drugs** 29 (2011) 1465–1474.
21. Tevaarwerk, A.J., Holen, K.D., Alberti, D.B., Sidor, C., Arnott, J., Quon, C., Wilding, G. and Liu, G. Phase I trial of 2-methoxyestradiol NanoCrystal dispersion in advanced solid malignancies. **Clin Cancer Res.** 15 (2009) 1460–1465.
22. Newman, S.P., Ireson, C.R., Tutill, H.J., Day, J.M., Parsons, M.F., Leese, M.P., Potter, B.V.L., Reed, M.J. and Purohit, A. The role of 17beta-hydroxysteroid dehydrogenases in modulating the activity of 2-methoxyestradiol in breast cancer cells. **Cancer Res.** 66 (2006) 324–330.
23. Liu, Q., Jin, W., Zhu, Y., Zhou, J., Lu, M. and Zhang, Q. Synthesis of 3'-methoxy-E-diethylstilbestrol and its analogs as tumor angiogenesis inhibitors. **Steroids** 77 (2012) 419–423.
24. Chiche, J., Ilc, K., Laferriere, J., Trottier, E., Dayan, F., Mazure, N.M., Brahimi-Horn, M.C. and Pouysségur, J. Hypoxia-inducible carbonic anhydrase IX and XII promote tumor cell growth by counteracting acidosis through the regulation of the intracellular pH. **Cancer Res.** 69 (2009) 358–368.

25. Visagie, M.H. and Joubert, A.M. In vitro effects of 2-methoxyestradiol-bis-sulfamate on reactive oxygen species and possible apoptosis induction in a breast adenocarcinoma cell line. **Cancer Cell Int.** 11 (2011) 43–49.
26. Supuran, C.T. and Scozzafava, A. Carbonic anhydrases as targets for medicinal chemistry. **Bioorg. Med. Chem.** 15 (2007) 4336–4350.
27. Genis, C., Sippel, K.H., Case, N., Cao, W., Avvaru, B.S., Tartaglia, L.J., Govindasamy, L., Tu, C., Agbandje-McKenna, M., Silverman, D.N., Rosser, C.J. and McKenna, R. Design of a carbonic anhydrase IX active-site mimic to screen inhibitors for possible anticancer properties. **Biochemistry** 48 (2009) 1322–1331.
28. Stander, B.A., Joubert, F., Tu, C., Sippel, K.H., McKenna, R. and Joubert, A.M. In vitro evaluation of ESE-15-ol, an estradiol analogue with nanomolar antimitotic and carbonic anhydrase inhibitory activity. **PLoS One** 7 (2012) e52205–e52215.
29. Leese, M.P., Leblond, B., Newman, S.P., Purohit, A., Reed, M.J. and Potter, B.V. Anti-cancer activities of novel D-ring modified 2-substituted estrogen-3-O-sulfamates. **J. Steroid Biochem. Mol. Biol.** 94 (2005) 239–251.
30. Chander, S.K., Foster, P.A., Leese, M.P., Newman, S.P., Potter, B.V., Purohit, A. and Reed, M.J. In vivo inhibition of angiogenesis by sulfamoylated derivatives of 2-methoxyoestradiol. **Br. J. Cancer** 96 (2007) 1368–1376.
31. Visagie, M.H. and Joubert, A.M. The in vitro effects of 2-methoxyestradiol-bis-sulfamate on cell numbers, membrane integrity and cell morphology, and the possible induction of apoptosis and autophagy in a non-tumorigenic breast epithelial cell line. **Cell. Mol. Biol. Lett.** 15 (2010) 564–581.
32. Stander, B.A., Joubert, F., Tu, C., Sippel, K.H., McKenna, R. and Joubert, A.M. Signaling pathways of ESE-16, an antimitotic and anticarbonic anhydrase estradiol analog, in breast cancer cells. **PLoS One** 8 (2013) e53853–e53871.
33. Mqoco, T., Marais, S. and Joubert, A. Influence of estradiol analogue on cell growth, morphology and death in esophageal carcinoma cells. **Biocell** 34 (2010) 113–120.
34. Stander, X.X., Stander, B.A. and Joubert, A.M. In vitro effects of an in silico-modelled 17-beta-estradiol derivative in combination with dichloroacetic acid on MCF-7 and MCF-12A cells. **Cell. Prolif.** 44 (2011) 567–581.
35. Stander, B.A., Marais, S., Vorster, C.J. and Joubert, A.M. In vitro effects of 2-methoxyestradiol on morphology, cell cycle progression, cell death and gene expression changes in the tumorigenic MCF-7 breast epithelial cell line. **J. Steroid Biochem. Mol. Biol.** 119 (2010) 149–160.
36. Kanzawa, T., Kondo, Y., Ito, H., Kondo, S. and Germano, I. Induction of autophagic cell death in malignant glioma cells by arsenic trioxide. **Cancer Res.** 63 (2003) 2103–2108.
37. Knizhnik, A.V., Roos, W.P., Nikolova, T., Quiros, S., Tomaszowski, K.H., Christmann, M. and Kaina, B. Survival and death strategies in glioma cells:

autophagy, senescence and apoptosis triggered by a single type of temozolomide-induced DNA damage. **PLoS One** 8 (2013) e55665–e55676.
38. Moriya, S., Che, X.F., Komatsu, S., Abe, A., Kawaguchi, T., Gotoh, A., Inazu, M., Tomoda, A. and Miyazawa, K. Macrolide antibiotics block autophagy flux and sensitize to bortezomib via endoplasmic reticulum stress-mediated CHOP induction in myeloma cells. **Int. J. Oncol.** 42 (2013) 1541–1550.
39. Taylor, J.P., Tanaka, F., Robitschek, J., Sandoval, C.M., Taye, A., Markovic-Plese, S. and Fischbeck, H. Aggresomes protect cells by enhancing the degradation of toxic polyglutamine-containing protein. **Hum. Mol. Genet.** 12 (2003) 749–757.
40. Garcia-Mata, R., Gao, Y.S. and Sztul, E. Hassles with taking out the garbage: aggravating aggresomes. **Traffic** 3 (2002) 388–396.
41. Simms-Waldrip, T., Rodriguez-Gonzalez, A., Lin, T., Ikeda, A.K., Fu, C. and Sakamoto, K.M. The aggresome pathway as a target for therapy in hematologic malignancies. **Mol. Genet. Metab.** 94 (2008) 283–286.
42. Nkandeu, D.S., Mqoco, T.V., Visagie, M.H., Stander, B.A., Wolmarans, E., Cronje, M.J. and Joubert, A.M. In vitro changes in mitochondrial potential, aggresome formation and caspase activity by a novel 17-beta-estradiol analogue in breast adenocarcinoma cells. **Cell. Biochem. Funct.** 31 (2013) 566–574.
43. Bialik, S., Zalckvar, E., Ber, Y., Rubinstein, A.D. and Kimchi, A. Systems biology analysis of programmed cell death. **Trends Biochem. Sci.** 35 (2010) 556–564.
44. Pradelli, L.A., Beneteau, M. and Ricci, J.E. Mitochondrial control of caspase-dependent and -independent cell death. **Cell. Mol. Life. Sci.** 67 (2010) 1589–1597.
45. Wang, C. and Klionsky, D.J. The Molecular Mechanism of Autophagy. **Mol. Med.** 9 (2003) 65–76.
46. Tanida, I., Ueno, T. and Kominami, E. LC3 and Autophagy. **Methods Mol. Biol.** 445 (2008) 77–88.
47. Zaarur, N., Meriin, A.B., Gabai, V.L. and Sherman, M.Y. Triggering aggresome formation. Dissecting aggresome-targeting and aggregation signals in synphilin 1. **J. Biol. Chem.** 283 (2008) 27575–27584.
48. Hsieh, Y.C., Athar, M. and Chaudry, I.H. When apoptosis meets autophagy: deciding cell fate after trauma and sepsis. **Trends Mol. Med.** 15 (2009) 129–138.
49. Thorburn, A. Apoptosis and autophagy: regulatory connections between two supposedly different processes. **Apoptosis** 13 (2008) 1–9.
50. Maiuri, M.C., Zalckvar, E., Kimchi, A. and Kroemer, G. Self-eating and Self-killing: crosstalk between autophagy and apoptosis. **Mol. Cell Biol.** 8 (2007) 741–752.